Available online at www.sciencedirect.com
SCIENCE DIRECT®
Journal of Nuclear Materials 329–333 (2004) 47–55
journal of nuclear materials
www.elsevier.com/locate/jnucmat

# Recent progress on development of vanadium alloys for fusion

R.J. Kurtz [a,*], K. Abe [b], V.M. Chernov [c], D.T. Hoelzer [d], H. Matsui [e], T. Muroga [f], G.R. Odette [g]

[a] *Pacific Northwest National Laboratory, P.O. Box 999, Richland, WA 99352, USA*
[b] *Department of Quantum Science and Energy Engineering, Tohoku University, Sendai 980-8579, Japan*
[c] *Bochvar Research Institute of Inorganic Materials, P.O. Box 369, Moscow, Russia*
[d] *Oak Ridge National Laboratory, P.O. Box 2008, Oak Ridge, TN 37831, USA*
[e] *Institute for Materials Research, Tohoku University, Sendai 980-8577, Japan*
[f] *National Institute for Fusion Science, Oroshi, Toki, Gifu 509-5292, Japan*
[g] *Department of Mechanical and Environmental Engineering, University of California at Santa Barbara, Santa Barbara, CA 93106, USA*

**Abstract**

Considerable progress has been made toward development of vanadium alloys for fusion. Much of the recent research has focused on vanadium alloys containing 4–5% Cr and 4–5% Ti, but a number of alternative compositions and processing routes have been explored in an effort to achieve improved performance. The goal of this paper is to review significant new results and to highlight critical issues that remain for future research. Progress in understanding the influence of interstitial impurities on microstructural evolution in both thermal and radiation environments are covered. The current state of knowledge of hardening and embrittlement of vanadium alloys in response to neutron irradiation is reviewed. Atomic-scale computer simulations to elucidate fundamental irradiation damage mechanisms are presented. The thermal and irradiation creep behavior of V–4Cr–4Ti is summarized along with an overview of the effects of He on tensile properties.


## 1. Introduction

It has been long recognized that V alloys are attractive candidate materials for fusion power system structural components due to their low induced activation characteristics coupled with high-temperature strength and high thermal stress factor. As noted in recent reviews [1–3] research over the past several years has successfully resolved many of the significant feasibility issues associated with use of V alloys in fusion first-wall/blanket structures. The emphasis of the worldwide V alloy development effort has been on the V–Cr–Ti system, with an alloy containing 4–5% Cr and 4–5% Ti serving as a reference composition in many research programs. This paper highlights recent progress on V alloys with regard to (1) atomistic studies of point defect behavior, (2) understanding microstructural evolution under variable temperature irradiation conditions, (3) assessing hardening and embrittlement following low-temperature irradiation, (4) determining thermal and irradiation creep rates, (5) evaluating the effects of He on tensile and creep deformation and (6) exploration of alternative alloy compositions for improved performance. Critical issues that require further research and development are described.

## 2. Atomistic studies of point defect behavior

Point defects, such as self-interstitial atoms (SIA) and vacancies, are produced in abundance when V alloys are irradiated with neutrons. Evolution of the microstructure, and therefore the properties of the material, is controlled by how these defects migrate through the

* Corresponding author. Tel.: +1-509 373 7515; fax: +1-509 376 0418.
*E-mail address:* rj.kurtz@pnl.gov (R.J. Kurtz).

0022-3115/$ - see front matter © 2004 Elsevier B.V. All rights reserved.
doi:10.1016/j.jnucmat.2004.04.299

lattice and interact with one another or with sinks such as dislocations, grain boundaries and other internal interfaces. Therefore, knowledge of the properties, formation and migration mechanisms of point defects and defect clusters is essential for developing robust models of radiation damage. Atomistic simulations play a key role in developing this information. The reliability of atomistic simulations depends largely on the efficacy of the interatomic potential utilized. Recently two new V potentials [4–6] have been developed in an effort to provide an improved description of the atom interactions in this metal. One of the potentials [4,5] uses the Finnis–Sinclair (FS) formalism. That potential was derived from an extensive set of first-principles calculations of six different SIA geometries and vacancies. The first-principles calculations revealed that the $\langle 1\,1\,1\rangle$ dumbbell is the most stable SIA in V with a formation energy of about 3.1 eV. The other potential [6] uses the modified embedded atom method (MEAM) developed by Baskes [7] to represent V. An important aspect of MEAM is that it attempts to account for the directional bonding characteristics of transition metals with partially filled d-orbitals. Satou et al. [6] refit several of the MEAM parameters derived by Baskes [7] to produce a new potential for V with elevated temperature elastic constants that are in better agreement with experimental values.

Zepeda-Ruiz and co-workers [8,9] have utilized the new FS V potential to study the temperature and orientation dependence of the threshold displacement energy (TDE). Molecular dynamics simulations were performed to determine the minimum kinetic energy transferred by a primary knock-on atom to a lattice atom that resulted in the formation of a stable Frenkel pair. They found a minimum TDE of 13 eV corresponding to displacements along a $\langle 1\,0\,0\rangle$ direction. The maximum TDE of 51 eV was observed in a direction close to $\langle 1\,1\,0\rangle$. The possibility for a larger TDE could not be excluded since the simulations did not span all possible angles. The TDE is essentially independent of temperature since the magnitude of the TDE is much greater than thermal energies. Comparison of the TDE in V with experimental values for Fe and Mo revealed that the directional anisotropy is comparable in Mo but the TDE ordering in $\langle 1\,1\,0\rangle$ and $\langle 1\,1\,1\rangle$ orientations is different in Fe.

Zepeda-Ruiz and co-workers [10,11] also investigated the character of SIA loops in V using the new FS potential. Their simulations showed that SIA dislocation loops with $\frac{a}{2}\langle 1\,1\,1\rangle$ Burgers vectors were the lowest energy configuration in V and migrated rapidly along their $\langle 1\,1\,1\rangle$ glide cylinder. Dislocation loops with $\frac{a}{2}\langle 1\,1\,0\rangle$ and $a\langle 1\,0\,0\rangle$ Burgers vectors easily rotated into $\frac{a}{2}\langle 1\,1\,1\rangle$ orientations at low temperatures during relaxation of the simulation cell. In contrast to Fe, where a metastable $a\langle 1\,0\,0\rangle$ loop is very close in energy to the ground-state $\frac{a}{2}\langle 1\,1\,1\rangle$ orientation, constrained $a\langle 1\,0\,0\rangle$ loops in V possess much higher formation energies than $\frac{a}{2}\langle 1\,1\,1\rangle$ loops, and the energy difference increases with the size of the loop. Simulations were also performed to explore the interaction of two mobile $\frac{a}{2}\langle 1\,1\,1\rangle$ clusters in V. The intersection of $\frac{a}{2}\langle 1\,1\,1\rangle$ loops on different glide cylinders has been proposed as a possible mechanism for $a\langle 1\,0\,0\rangle$ loop formation in Fe. Similar work carried out on V indicate that $a\langle 1\,0\,0\rangle$ junctions form during the intersection of two $\frac{a}{2}\langle 1\,1\,1\rangle$ loops, but the junction has low thermal stability and rotates into a $\frac{a}{2}\langle 1\,1\,1\rangle$ orientation at temperatures between 327 and 527 °C.

Finally, Han et al. [12] and Zepeda-Ruiz et al. [13] examined SIA diffusion in V as a function of temperature to determine the predominant mechanisms. Their MD results showed that $\langle 1\,1\,1\rangle$ oriented dumbbells migrate rapidly along $\langle 1\,1\,1\rangle$ directions. The SIA migration mechanism was found to be temperature dependent. At low to intermediate temperatures (−173 to 327 °C) the SIA executed a 1D random walk along a $\langle 1\,1\,1\rangle$ direction. Above 427 °C the SIA began to make infrequent rotations from one $\langle 1\,1\,1\rangle$ direction to another $\langle 1\,1\,1\rangle$ direction. This resulted in 3D like migration trajectory that consisted of long segments of 1D diffusion punctuated by abrupt reorientations. As the temperature increased the frequency of rotation events increased and the lengths of the 1D segments decreased. The apparent activation energy for SIA diffusion increased with increasing temperature. Detailed study of their simulation results revealed that the intrinsic activation energy for SIA diffusion is not temperature dependent, but that SIA jumps are correlated and the correlation factor is highly temperature dependent below 527 °C.

## 3. Microstructural evolution

A recent emphasis of microstructural evolution studies has been an exploration of the effects of varying irradiation temperature. It is well known that the irradiation temperature can have a significant impact on microstructural development [14]. Variable irradiation temperature can result in significant changes in the microstructure, especially when the temperature excursion occurs between the nucleation and growth regimes [15]. At lower temperatures nucleation of defect clusters is maximized, while at higher temperatures cluster growth and coarsening is maximized. These effects have been explored in neutron and ion irradiations to low doses but not, until recently, to higher dose levels. One of the major tasks of the Japan–US Fusion Cooperation Program (JUPITER) was to investigate the effects of varying irradiation temperature on V alloys to a dose of 4 dpa [16].

In a recent paper Zinkle et al. [17] showed a moderate enhancement of radiation-induced precipitates and dislocation loops for V–4Cr–4Ti undergoing varying tem-

perature irradiation 360/520 °C compared to irradiation at a constant temperature of 520 °C. The varying temperature irradiation consisted of eight cycles in which the initial 10% was conducted at 360 °C and the remaining 90% at 520 °C. Varying temperature conditions produced precipitates of finer size and greater number density than under constant temperature conditions, but overall the quantitative effect of the low-temperature excursions was relatively small. Zinkle et al. [17] suggested that more pronounced differences might have been observed had the low-temperature portion of each cycle been below the recovery stage V temperature. More recently Watanabe et al. [18] examined pure V and four model V alloys from the same experiment, irradiated under the same conditions. These investigators found that varying temperature enhanced void formation in pure V and V–5Cr compared to isothermal irradiation, and a small number of ⟨1 0 0⟩ oriented carbides were observed in pure V. For V–4Cr–4Ti and V–5Ti alloys a higher density of Ti oxides was produced under varying temperature but, as noted by Zinkle et al. [17] the effects of varying temperature were not large. It should be noted that while recent work has not shown substantial microstructural differences between varying temperature and isothermal irradiation conditions, some differences were observed. Such differences may be exacerbated by selection of different temperature extremes or by performing irradiations to higher doses [19]. A better understanding of the effects of varying irradiation temperature will require additional experiments but, more importantly, the development of quantitative models to predict material performance under complex irradiation conditions.

Another aspect of V alloy metallurgy that has received increased attention in recent years is the interaction of V with interstitial impurities such as C, O and N. Several recent studies [20–22] have shown that most precipitates result from reaction of V or solute atoms with these impurities. These precipitates impede dislocation motion increasing the strength of the alloy. Ti lowers the mobility of the interstitials and reacts to form precipitates at $>\sim$600 °C under thermal annealing and $>\sim$300 °C under neutron irradiation. Globular Ti-(CON) precipitates appear above $\sim$1000 °C. The solvus temperature for globular precipitates is between 1200 and 1300 °C. Following dissolution the interstitial content can be redistributed into a high number density of nanosize {100} plates by controlled precipitation. The precipitate crystal structure is FCC for both {100} plate and globular morphologies. The interstitial concentration varies considerably for {100} plate type precipitates. A conclusion of these investigations is that a better understanding of precipitate nucleation and growth is needed along with an increased knowledge of the range of interstitial solubility. To gain a better understanding of the effects of interstitial impurities on irradiated properties a special set of V alloys [23] with carefully controlled levels of C, O and N has been included in an upcoming JUPITER irradiation experiment.

## 4. Hardening and embrittlement

Neutron irradiation at temperatures at and below 400 °C gives rise to hardening and loss of uniform strain [24]. This temperature limit may increase with increasing dose. Hardening and loss of ductility become more pronounced with increasing dose and decreasing irradiation temperature, and are accompanied by varying degrees of flow localization, as evidenced by the formation of dislocation channels in the irradiated microstructure [25]. However, recent finite element modeling of the deformation of flat tensile specimens has demonstrated that the loss of uniform strain can be affected by both an increase in yield strength as well as a decrease in work hardening [26]. Engineering stress strain curves showing no uniform strain and the onset of necking coincident with yield can be generated with constitutive equations that exhibit a gradual yield drop followed by a strain hardening regime. Moreover, the modeling results show that significant irradiation hardening can persist to high strain. Ongoing modeling work will benefit from calibration against data from new techniques that permit strain mapping in all three dimensions during uniform and localized strain, as well as specimen and test designs that explore stress states other than uniaxial tension [27]. The modeling effort also provides a guide for future experiments to explore and understand the effects and consequences of microscopic flow localization on macroscopic deformation behavior.

While considerable information on irradiation hardening of V alloy base metals is available there is a corresponding lack of data on weld metal. Nagasaka et al. [28] recently completed an exploratory study of the effects of low-dose neutron-irradiation on the impact properties of NIFS Heat-2 weld metal. Miniature Charpy impact specimens of V–4Cr–4Ti base and weld metal were irradiated at 290 °C to a dose of 0.08 dpa in the JMTR. Weld metal specimens hardened more than base metal specimens, but the effects of neutron irradiation were reduced if a post-weld heat treatment in the range 600–950 °C was applied prior to irradiation. The predominant radiation defects found in both base and weld metal microstructures were identified as dislocation loops. The higher density of loops found in weld metal compared to base metal did not account for all of the hardness difference. The authors postulated an additional component of hardening associated with decoration and stabilization of dislocation loops by interstitial impurities released into solution by dissolution of Ti-(CON) precipitates during welding.

In an effort to improve high-temperature strength and oxidation resistance of V–*x*Cr–4Ti alloys, Sakai et al. [29] performed a study of the effects of Cr additions on fracture properties. The Cr content varied from 4% to 20%. Changes in the ductile-to-brittle transition temperature (DBTT) were correlated with the Cr content and precipitate microstructures produced during heat treatments following cold working. Their research shows that the DBTT is about −190 °C when the Cr content is <10% but rises sharply to −30 °C for alloys with more than 10% Cr. The increased DBTT was associated, in part, to increased flow stress due to solid solution strengthening. The sharp rise in DBTT for Cr >10% was also related to a substantial increase in large diameter (>400 nm) Ti-(CON) and $TiO_2$ precipitates. This work nicely illustrates the difficulty of altering the alloy composition to improve high-temperature strength at the expense of degrading fracture resistance. The process of optimizing V alloy composition and heat treatment procedures for best performance in a radiation environment is certainly not simple or straightforward.

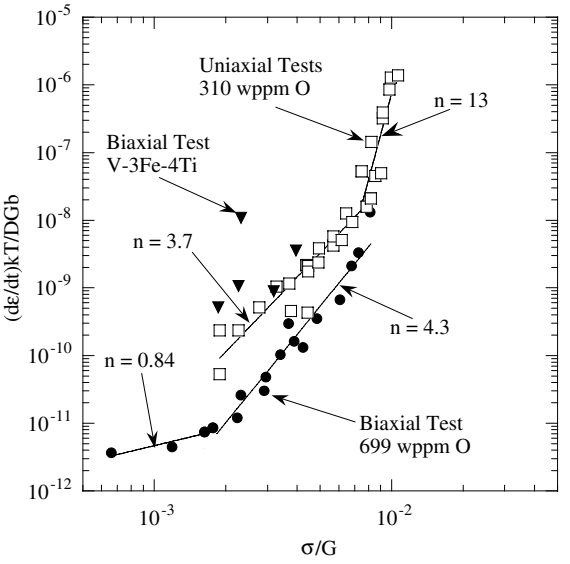


Fig. 1. Stress dependence of the normalized effective mid-wall creep strain for unirradiated V–4Cr–4Ti and V–3Fe–4Ti. Normalized stresses are Von Mises effective stresses for biaxial tests. The initial oxygen concentration of the uniaxial and biaxial test specimens was 310 and 699 wppm, respectively.

## 5. Thermal and irradiation creep

A significant amount of thermal creep data on pure vanadium and various V–Cr–Ti alloys was generated several years ago [30–36]. These data demonstrate that Cr significantly increases the creep resistance of V. More recently, several studies have characterized the thermal creep performance of V–4Cr–4Ti in vacuum and liquid Li [37–44]. Both uniaxial [37,38] and biaxial [41,42] tests were performed in vacuum with different starting concentrations of interstitial O. The results show that the normalized secondary creep rate ($\dot{\varepsilon}kT/DGb$) is power-law dependent on stress with a stress exponent of ~4 at normalized stresses ($\sigma/G$) greater than 0.002. The activation energy for creep between 700 and 800 °C is about 300 kJ/mol, which is similar to the activation energy for self-diffusion in pure V suggesting that in this regime of temperature and stress the predominant creep mechanism appears to be climb-assisted dislocation motion. Limited data at the same temperatures but lower stresses indicates that the creep mechanism may change since the stress exponent appears to decrease to about unity (Fig. 1).

The effect of oxygen on creep strength was convincingly demonstrated in several experiments. The creep rates measured in vacuum with tensile samples [37] containing about 310 wppm O were several times greater than creep rates from pressurized tubes [41,42] with an initial O concentration of about 700 wppm. Similarly, the creep rates measured in Li were higher than those in vacuum [39,40,43]. This is consistent with the vacuum creep data since Li has a higher affinity for O than V and will, after long exposure times, lower the O level in the alloy. Recently Fukumoto et al. [38] and Koyama et al. [44] utilized a novel Zr-foil gettering heat treatment to reduce interstitial O and N concentrations to very low levels in V–4Cr–4Ti and V–10Cr–5Ti sheet stock. Tensile specimens prepared from these highly purified alloys were used to study dynamic strain aging (DSA) and creep properties. The results of these investigations show that high-temperature tensile and creep strengths decrease substantially as interstitial O decreases. Further, DSA was suppressed by O removal as evidenced by a large decrease in the height of post-yield load serrations. Contrary to expectation, the temperature range over which a negative strain rate sensitivity parameter was observed increased rather than decreased suggesting a larger temperature window for heterogeneous deformation. An effort to resolve this inconsistency will be the subject of a future investigation on highly purified unalloyed V.

The maximum operating temperature limit for V alloys in design studies is typically assumed to be about 700 °C [45]. Alternately, it has been suggested that V alloys might be capable of operation at 750 °C [46]. The thermal creep database may be used to derive an estimate of the limiting stress to avoid creep damage in a structure for a specific time at temperature. A Larsen–Miller parameter plot of the time to reach 1% creep strain is presented in Fig. 2. A creep strain limit of 1% is representative of structural design criteria for first-wall

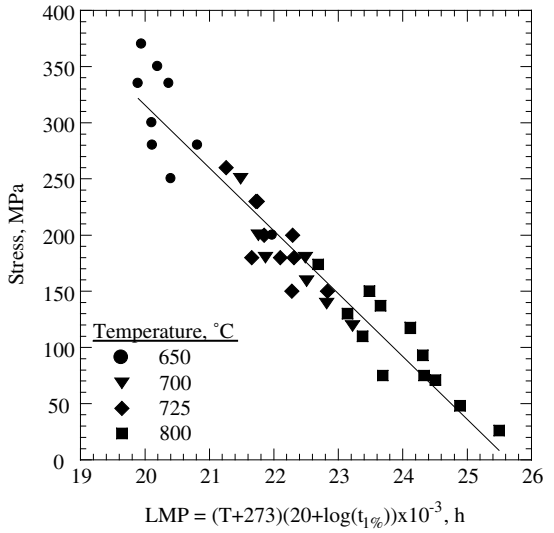


Fig. 2. Larsen–Miller parameter plot (time to reach 1% creep strain) for V–4Cr–4Ti tested in vacuum (uniaxial and biaxial specimens) at the indicated temperatures.

components for a fusion power system [47]. Selecting a first-wall life of $10^5$ h yields limiting stresses of 74 MPa at 700 °C and only 4 MPa at 750 °C from the curve fit to the data. The coolant pressure for a V/Li system is about 0.5 MPa [47], which should result in relatively low applied loads in the first-wall. It is important to note, however, that detailed stress analyses have not been performed in recent V/Li design studies, therefore all the expected loadings are not well known. The creep data indicates that an attractive design may be feasible at 700 °C, but probably not at 750 °C. Improving the thermal creep strength would add margin at 700 °C to account for uncertainties in anticipated loadings and perhaps expand the design window to higher temperatures.

The irradiation creep database for the V–Cr–Ti alloy system is very sparse. Only a few experiments have been performed between 300 and 500 °C to damage levels of a few dpa. There is a significant divergence in effective strain rate at effective stresses greater than about 125 MPa. A Russian study suggests a bilinear relationship between the effective irradiation creep strain rate and the effective stress, but such behavior was not observed in more recent experiments carried out under the auspices of the JUPITER program [48]. More data will be forthcoming from experiments recently inserted in the HFIR and JOYO reactors but dose levels will again be on the order of only 5–7 dpa.

For the future additional thermal creep experiments are warranted to examine ways to improve performance through alternative compositions and microstructures without degrading properties such as fracture toughness. More work is needed to define the irradiation creep characteristics of these alloys as there is almost a complete lack of data at any significant dose. Further, the effect of alloy composition and heat treatment on irradiation creep remains to be explored.

## 6. Helium embrittlement

The upper temperature limit for V alloys is most probably determined by the effect of gaseous transmutants such as He on creep rupture behavior in the 600–800 °C temperature regime. The most realistic studies to perform involve simultaneous creep deformation and introduction of displacement damage and He at fusion relevant rates (~4 appm He/dpa). In the absence of a 14 MeV volumetric neutron source these types of experiments are exceedingly difficult to perform and consequently are seldom done. More often, pre-implanting a tensile specimen with a particular quantity of He and then conducting a tensile test at a strain rate ranging from $10^{-3}$ to $10^{-4}$ $s^{-1}$ have been used to characterize the effect of He on elevated temperature mechanical properties. Occasionally pre-implanted tensile specimens have also been neutron-irradiated to explore the concomitant effects of He and radiation damage on tensile properties.

The effect of He on tensile properties has been studied over a broad range of temperatures for a variety of V alloys [49–57]. Fig. 3 shows the temperature dependence of the normalized tensile ductility for He concentrations ranging from 14 to 480 appm. The normalized ductility is the total tensile elongation for a He-implanted specimen, $e_{tot}$(He), divided by the total tensile elongation of a He-free specimen tested at the same temperature, $e_{tot}$(ref). In all these experiments He was pre-implanted prior to performing the tensile test by either cyclotron irradiation [49–52,55–57] or by a modified tritium trick technique [53,54] where the implantation temperature is typically quite low relative to the tensile test temperature. Matsui et al. [58] have suggested that the He-implantation method can significantly affect the tensile test results, but the data in Fig. 3 do not display a trend indicating that one implantation technique leads to systematically lower ductility than another. Normalized tensile ductilities with values near unity indicate no significant effect of He. Close inspection of the data reveals that He at levels of $\leqslant 25$ appm did not significantly degrade tensile ductility at any test temperature. When the He concentration was $\geqslant 25$ appm tensile ductility was substantially reduced at temperatures $\geqslant 650$ °C. A puzzling feature of the data is the apparent effect of He at temperatures around 420–450 °C. Low normalized tensile ductility in this temperature regime is evident for the Cr bearing V alloys only, suggesting that He may be more deleterious for high strength alloys.

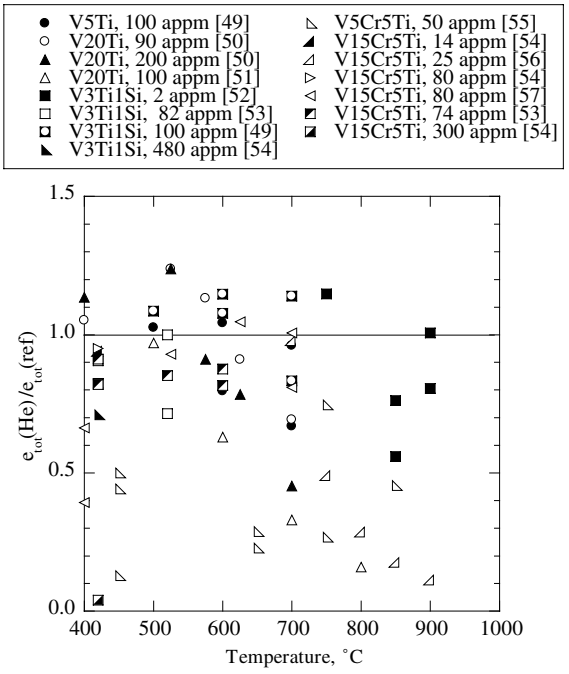


Fig. 3. Temperature dependence of the normalized total elongation for several V alloys pre-implanted with He. Implantation was performed by cyclotron injection or a modified tritium trick technique.

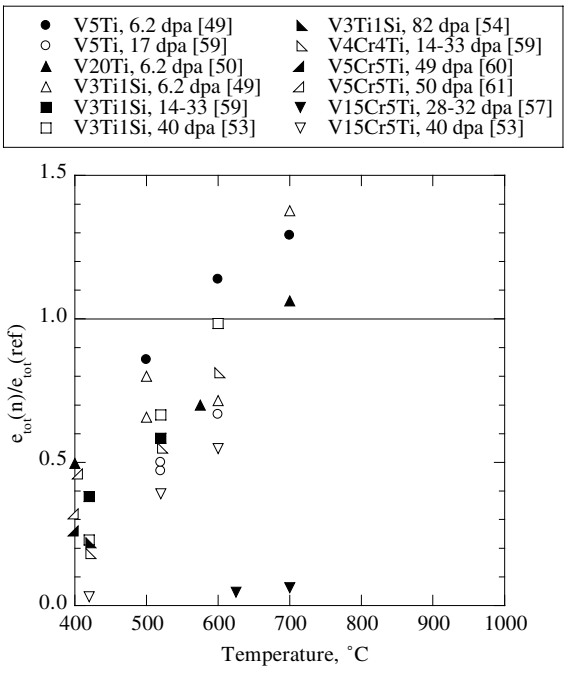


Fig. 4. Temperature dependence of the normalized total elongation for several He-free, neutron-irradiated V alloys. The irradiation and tensile test temperatures were the same in all cases.

It is instructive to also examine the effect of neutron irradiation on tensile ductility for He-free and pre-implanted specimens to determine the relative contributions of He and neutron irradiation on ductility reduction. Fig. 4 gives a plot of the temperature dependence of the normalized tensile ductility for He-free V alloys neutron irradiated to doses ranging from about 6 to 82 dpa [49,50,53,54,57,59–61]. The data exhibits some scatter but there is a clear trend that the effects of neutron irradiation on tensile ductility are minimal for irradiation temperatures $\geqslant 650$ °C. A similar trend is found for specimens pre-implanted with He and then irradiated (Fig. 5) [49,50,53,54,57,59–61]. These results indicate that He pre-implantation did not further reduce tensile ductility beyond that already caused by neutron irradiation. Results from the dynamic helium charging experiment (DHCE) [59], which closely simulates the actual fusion environment because He and neutron damage are produced concurrently, displays the same trend. It is clear from the data in Figs. 3–5 that over the temperature range 400–600 °C displacement damage is the largest contributor to loss of ductility. It is important to recognize, however that none of the experiments mentioned above exactly simulated the environment that a structural material will face in a real fusion power system, namely high-temperature, time-dependent deformation in the presence of simultaneous He production and displacement damage so the relative importance of each of these variables may be different for a real power system.

Recently, Chuto et al. [62] explored the effect of pre-implanted He on the creep properties of V–4Cr–4Ti. It was anticipated that the effects of He would be more pronounced at strain rates typical of creep deformation, although data by van Witzenburg and Scheurer [63] indicate that V–5Ti pre-implanted with up to 100 appm He and neutron irradiated to 4.5 dpa show little sensitivity of the total elongation to strain rate over the range $10^{-6}$–$10^{-3}$ $s^{-1}$. Helium was cyclotron implanted by Chuto et al. [62] at 700 °C followed by creep testing at the same temperature. Creep testing of He-free control samples exposed to the same thermal history as the implanted ones was also performed. Interestingly, the creep strength of the He implanted specimens was significantly better than the He-free samples, even though the fracture surfaces of the implanted specimens were 5–15% intergranular. The superior creep performance of the He-implanted specimens was attributed to irradiation strengthening, but this explanation lacks appeal since radiation damage associated with the 700 °C implantation should be minimal. Matrix strengthening from a fine dispersion of He clusters seems more likely, but microstructural characterization remains to be performed.

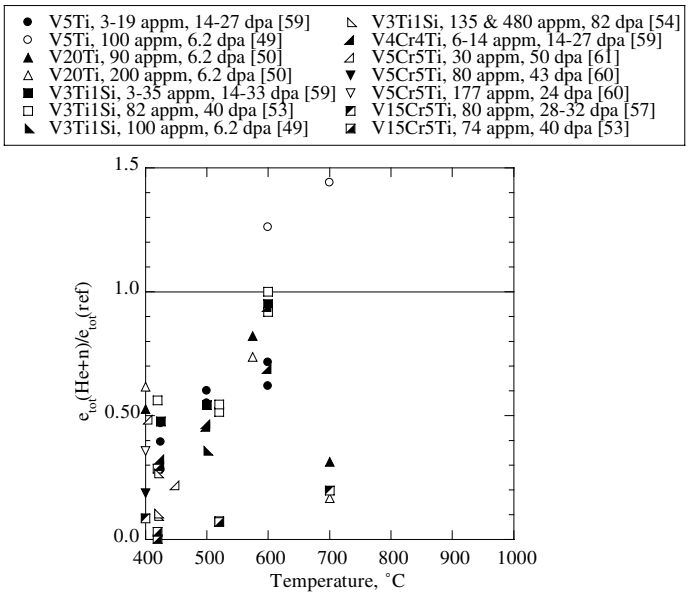


Fig. 5. Temperature dependence of the normalized total elongation for several V alloys pre-implanted with He and then neutron-irradiated. Implantation was performed by cyclotron injection or a modified tritium trick technique. The irradiation and tensile test temperatures were the same in all cases.

The effect of He on microstructural development still needs to be addressed intensely. Work performed to date has lead to qualitative understanding of basic effects, but accurate quantitative evaluations are not possible due to insufficient data. A 14 MeV fusion neutron source is absolutely essential to acquiring the needed data, but progress may be possible with simulation techniques such as the DHCE.

## 7. Advanced alloys

While V alloys offer many attractive properties for fusion applications there is growing recognition that the reference composition, V–4Cr–4Ti, may not be fully adequate to meet the stringent requirements of an advanced power system in terms of resistance to He embrittlement and creep damage. Consequently, alternative compositions are being considered to improve the low-temperature radiation resistance and high-temperature strength. Chen et al. [64] have recently studied the properties of V-based alloys containing 6–8 wt% W. A broad range of properties were investigated including recovery and recrystallization behavior, the room temperature tensile properties, the solid solution strengthening efficiency of various elements, the susceptibility to H embrittlement and oxidation kinetics in air from 400 to 600 °C. The recovery and recrystallization behavior of V–W alloys not including Ti was similar to unalloyed V, while V–W alloys including Ti gave results similar to V–4Cr–4Ti. The N concentration affected the temperature for onset of recovery in a V–6W–1Ti alloy. Increasing the N concentration from 5 to 30 wppm was sufficient to increase the temperature for onset of recovery by about 100 °C. Tungsten, on a per atom basis, was observed to be a more effective strengthener than either Ti or Cr. The room temperature tensile properties of the V–W alloys examined by Chen et al. were equal to or better than a V–4Ti alloy. The addition of W did not influence the H embrittlement behavior. Although Ti tends to enhance H absorption, it appears to be the key element for imparting high resistance to H embrittlement. Parabolic oxidation kinetics were observed for all of the alloys investigated by Chen et al. This result is consistent with an earlier study [65] that demonstrated the oxidation kinetics depend strongly on the O partial pressure. At high O partial pressures parabolic oxidation kinetics are found and low O partial pressures linear kinetics are obeyed. From an operational point of view the most relevant environmental conditions are low O partial pressures and temperatures of about 700 °C.

It is well known that V alloys are readily embrittled by neutron irradiation at temperatures below about 400 °C [2,3]. Since grain and interphase boundaries act as efficient sinks for point defects produced under irradiation, alloys possessing ultra-fine grains and fine-scale particles may be more resistant to radiation-induced embrittlement. To test this hypothesis, Kobayashi et al. [66] examined the effects of neutron irradiation on the microstructure and hardness of V alloys containing

small amounts of Y. Two V alloys with 1.6 and 2.6 wt% Y were prepared by mechanical alloying techniques. The microstructure of the unirradiated materials displayed a mixture of fine grains a few hundred nanometers in diameter along with a small amount of coarse grains a few micrometers in diameter. TEM disks prepared from these materials were irradiated in the JMTR at 290 °C to a dose of 0.25 dpa and at 800 °C to a dose of 0.7 dpa. The results of this study showed that formation of interstitial loops and voids was suppressed in fine grain regions. Hardness increases associated with low-temperature neutron irradiation (290 °C) were relatively modest (3–70 $H_v$) compared to conventional V alloys processed using ingot metallurgy procedures. Kobayashi et al., found that the ultra-fine grains were stable, only limited particle coarsening occurred at 800 °C, and grain miniaturization effectively suppressed formation of radiation-induced defects. Another potential benefit such microstructures may provide is increased resistance to He embrittlement. Higher dose irradiation data is needed to validate the efficacy of this approach for improving radiation resistance.

## 8. Critical issues for future research

While significant progress has been made toward development of V alloys for fusion applications there remain a number of critical issues that should receive attention in ongoing research programs. The present understanding of the influence of interstitial impurities such as C, O and N on tensile, creep and fracture properties is not sufficient. Low-temperature ($\leqslant 450$ °C) properties appear to be improved by removing C, O and N but high-temperature creep strength is reduced. Ideally, elements such as C, O and N should be considered as alloying elements in V, analogous to C in steel, rather than undesirable impurities. To achieve this state will require much better control of these elements.

Recent atomistic modeling studies have advanced our understanding of fundamental point defect behavior in V alloys, but more needs to be done to develop robust models of material behavior that offer predictive capability. Complex experiments such as variable temperature irradiations need further detailed microstructural characterization coupled with the development of appropriate models that enhance our understanding of the experimental observations.

Although not described in this paper, a lot of progress has been made in development of constitutive laws for unirradiated V alloys [27]. This methodology needs to be extended to irradiated material. Further, the effects of flow localization and the contribution of dynamic strain aging need to be included. Extension of the Master curve – $\Delta T$ and micromechanics approaches to characterize and predict the temperature dependence of fracture toughness for irradiated material should be a high priority. A complete fracture resistance model must also consider the impact of non-hardening embrittlement mechanisms driven by impurity-solute segregation, phase instabilities and the production of He and H. In addition, subcritical crack growth (fatigue and environmentally assisted) and the realities of actual service such as warm pre-stressing, shallow surface flaws, multiaxial/mixed mode loading, dynamic strain aging and creep relaxation will also play a role.

The thermal creep performance of V alloys may need improvement. The current reference alloy, V–4Cr–4Ti, may not posses adequate creep strength. There is a need to explore alternative alloying elements for improved creep performance and He management and some steps in this direction have already been taken [64,66]. Higher dose irradiation creep data and an understanding of the effects of alloy composition on irradiation creep is required. The effects of He and H on creep resistance, swelling and post-irradiation tensile properties over the range $600 \leqslant T \leqslant 800$ °C is needed. Development of an alloy with a multiphase microstructure may be needed for more efficient He management since the sink strength of V–4Cr–4Ti for He trapping may not be adequate.

## Acknowledgements

This work was performed, in part, under the auspices of the US Department of Energy, Office of Fusion Energy Sciences, under contract DE-AC06-76RLO1830.

## References

[1] T. Muroga, M. Gasparotto, S.J. Zinkle, Fus. Eng. Des. 61&62 (2002) 13.
[2] T. Muroga, T. Nagasaka, K. Abe, V.M. Chernov, H. Matsui, D.L. Smith, Z.-Y. Xu, S.J. Zinkle, J. Nucl. Mater. 307–311 (2002) 547.
[3] R.J. Kurtz, K. Abe, V.M. Chernov, V.A. Kazakov, G.E. Lucas, H. Matsui, T. Muroga, G.R. Odette, D.L. Smith, S.J. Zinkle, J. Nucl. Mater. 283–287 (2000) 70.
[4] S. Han, L.A. Zepeda-Ruiz, G.J. Ackland, R. Car, D.J. Srolovitz, Phys. Rev. B (2002) 220101(R).
[5] S. Han, L.A. Zepeda-Ruiz, G.J. Ackland, R. Car, D.J. Srolovitz, J. Appl. Phys. 93 (6) (2003) 3328.
[6] M. Satou, S. Yip, K. Abe, J. Nucl. Mater. 307–311 (2002) 1007.
[7] M.I. Baskes, Phys. Rev. B 46 (1992) 2727.
[8] L.A. Zepeda-Ruiz, S. Han, D.J. Srolovitz, R. Car, B.D. Wirth, Fusion Materials Semi-Annual Progress Report, DOE/ER-0313/34, 2003, p. 32.
[9] L.A. Zepeda-Ruiz, S. Han, D.J. Srolovitz, R. Car, B.D. Wirth,, Phys. Rev. B 67 (2003) 134114.
[10] L.A. Zepeda-Ruiz, J. Marion, B.D. Wirth, D.J. Srolovitz, Fusion Materials Semi-Annual Progress Report, DOE/ER-0313/34, 2003, p. 31.

[11] L.A. Zepeda-Ruiz, J. Marion, B.D. Wirth, Philos. Mag., in press.
[12] S. Han, R. Car, D.J. Srolovitz, L.A. Zepeda-Ruiz, Fusion Materials Semi-Annual Progress Report, DOE/ER-0313/33, 2003, p. 2.
[13] L.A. Zepeda-Ruiz, S. Han, G.J. Ackland, R. Car, D.J. Srolovitz, Fusion Materials Semi-Annual Progress Report, DOE/ER-0313/34, 2003, p. 30.
[14] M. Kiritani, J. Nucl. Mater. 160 (1988) 135.
[15] H. Matsui, in: Proceedings of the 6th IEA and JUPITER Joint Workshop on Vanadium Alloys for Fusion Energy Applications, Tucson, AZ, 2002.
[16] K. Abe, A. Kohyama, C. Namba, F.W. Wiffen, R.H. Jones, J. Nucl. Mater. 258–263 (1998) 2075.
[17] S.J. Zinkle, N. Hashimoto, D.T. Hoelzer, A.L. Qualls, T. Muroga, B.N. Singh, J. Nucl. Mater. 307–311 (2002) 192.
[18] H. Watanabe, T. Muroga, N. Yoshida, these Proceedings.
[19] N. Nita, T. Yamamoto, T. Iwai, K. Yasunaga, K. Fukumoto, H. Matsui, J. Nucl. Mater. 307–311 (2002) 398.
[20] N.J. Heo, T. Nagasaka, T. Muroga, H. Matsui, J. Nucl. Mater. 307–311 (2002) 620.
[21] D.T. Hoelzer, J. Bentley, in: Proceedings of the 6th IEA and JUPITER Joint Workshop on Vanadium Alloys for Fusion Energy Applications, Tucson, AZ, 2002.
[22] A. Nishimura, A. Iwahori, N.J. Heo, T. Nagasaka, T. Muroga, S.-I. Tanaka, these Proceedings.
[23] D.T. Hoelzer, A.F. Rowcliffe, L.T. Gibson, Fusion Materials Semi-Annual Progress Report, DOE/ER-0313/34, 2003, p. 22.
[24] R.J. Kurtz, R.H. Jones, E.E. Bloom, A.F. Rowcliffe, D.L. Smith, G.R. Odette, F.W. Wiffen, Nucl. Fus. 39 (11Y) (1999) 2055.
[25] P.M. Rice, S.J. Zinkle, J. Nucl. Mater. 258–263 (1998) 1414.
[26] G.R. Odette, M.Y. He, E.G. Donahue, P. Spaetig, T. Yamamoto, J. Nucl. Mater. 307–311 (2002) 171.
[27] G.E. Lucas, K. Abe, in: Proceedings of the 6th IEA and JUPITER Joint Workshop on Vanadium Alloys for Fusion Energy Applications, Tucson, AZ, 2002.
[28] T. Nagasaka, N.J. Heo, T. Muroga, A. Nishimura, H. Watanabe, M. Narui, K. Shinozaki, these Proceedings.
[29] K. Sakai, M. Satou, M. Fujiwara, K. Takanashi, A. Hasegawa, K.Abe, these Proceedings.
[30] K.R. Wheeler, E.R. Gilbert, F.L. Yaggee, S.A. Duran, Acta Metall. 19 (1971) 21.
[31] M. Shirra, KfK 2440, Kernforschungszentrum Karlsruhe, 1989.
[32] H. Boehm, M. Schirra, KfK 774, Kernforschungszentrum Karlsruhe, 1968.
[33] W. Pollack, R.W. Buckman, R.T. Begley, K.C. Thomas, E.C. Bishop, WCAP-3487-16, Westinghouse Electric Corporation, 1968.
[34] T. Kainuma, N. Iwao, T. Suzuki, R. Watanabe, J. Less Common Met. 86 (1982) 263.
[35] H.M. Chung, B.A. Loomis, D.L. Smith, in: US Contribution, 1994 Summary Report, Task T12: Compatibility and Irradiation Testing of Vanadium Alloys, ANL/FPP/TM-287, ITER/US/95/IV MAT 10, 1995, p. 87.
[36] J.R. Stewart, J.C. LaVake, S.S. Christopher, Data presented at an AEC/RDT Working Group Meeting, Ames, Iowa, 1968.
[37] K. Natesan, W.K. Soppet, A. Purohit, J. Nucl. Mater. 307–311 (2002) 585.
[38] K. Fukumoto, T. Yamamoto, N. Nakao, S. Takahashi, H. Matsui, J. Nucl. Mater. 307–311 (2002) 610.
[39] M.L. Grossbeck, J. Nucl. Mater. 307–311 (2002) 615.
[40] M.L. Grossbeck, Fusion Materials Semi-Annual Progress Report, DOE/ER-0313/31, 2001, p. 2.
[41] R.J Kurtz, A.M. Ermi, H. Matsui, Fusion Materials Semi-Annual Progress Report, DOE/ER-0313/31, 2001, p. 7.
[42] D.S. Gelles, Fusion Materials Semi-Annual Progress Report, DOE/ER-0313/31, 2001, p. 17.
[43] M.L. Grossbeck, R.J. Kurtz, L.T. Gibson, M.J. Gardner, Fusion Materials Semi-Annual Progress Report, DOE/ER-0313/32, 2002, p. 6.
[44] M. Koyama, K. Fukumoto, H. Matsui, these Proceedings.
[45] H. Matsui et al., Fus. Technol. 30 (1996) 1293.
[46] D.L. Smith, M.C. Billone, S. Majumdar, R.F. Mattas, D.K. Sze, J. Nucl. Mater. 258–263 (1998) 65.
[47] S. Majumdar, Fus. Eng. Des. 49&50 (2000) 19.
[48] H. Tsai, R.V. Strain, M.C. Billone, T.S. Bray, D.L. Smith, M.L. Grossbeck, K. Fukumoto, H. Matsui, Fusion Materials Semi-Annual Progress Report, DOE/ER-0313/27, 2000, p. 65.
[49] W. van Witzenburg, E. de Vries, ASTM STP 1125 (1992) 915.
[50] M.P. Tanaka, E.E. Bloom, J.A. Horak, J. Nucl. Mater. 103&104 (1981) 895.
[51] A.I. Ryazanov, V.M. Manichev, W. van Witzenburg, J. Nucl. Mater. 227 (1996) 304.
[52] K. Ehrlich, H. Boehm, in: Proceedings of the IAEA Conference on Radiation Damage in Reactor Materials 2, Vienna, Austria, 1969, p. 349.
[53] D.N. Braski, ASTM STP 956 (1987) 271.
[54] D.N. Braski, ASTM STP 1047 (1990) 161.
[55] M. Satou, H. Koide, A. Hasagawa, K. Abe, Sci. Rep. RITU A 45 (1997) 157.
[56] A.T. Santhanam, A. Taylor, S.D. Harkness, Nuc. Metall. 18 (1973) 302.
[57] M.L. Grossbeck, J.A. Horak, ASTM STP 956 (1987) 291.
[58] H. Matsui, M. Tanaka, M. Yamamoto, A. Hasagawa, K. Abe, ASTM STP 1175 (1993) 1215.
[59] M.C. Billone, Fusion Materials Semi-Annual Progress Report, DOE/ER-0313/23, 1997, p. 3.
[60] M. Satou, H. Koide, A. Hasegawa, K. Abe, H. Kayano, H. Matsui, J. Nucl. Mater. 233–237 (1996) 447.
[61] M. Satou, T. Chuto, H. Koide, A. Hasagawa, K. Abe, Mater. Res. Soc. Symp. Proc. 540 (1999) 591.
[62] T. Chuto, N. Yamamoto, J. Nagakawa, Y. Murase, these Proceedings.
[63] W. van Witzenburg, H. Scheurer, in: Proceedings of the Fourteenth Fusion Technology Symposium, Avignon, France, 1986, p. 987.
[64] J.M. Chen, T. Muroga, S.Y. Qiu, T. Nagasaka, W.G. Huang, M.J. Tu, Y. Chen, Y. Xu, Z.Y. Xu, these Proceedings.
[65] B.A. Pint, J.R. Distefano, J. Nucl. Mater. 307–311 (2002) 560.
[66] S. Kobayashi, Y. Tsuruoka, K. Nakai, H. Kurishita, these Proceedings.